Interpreting 750 GeV diphoton resonance as degenerate Higgs bosons in NMSSM with vector-like particles

Fei Wang [1], Wenyu Wang[2], Lei Wu[3], Jin Min Yang[4], and Mengchao Zhang[4]

[1] *School of Physics, Zhengzhou University, Zhengzhou 453000, China*

[2] *Institute of Theoretical Physics, College of Applied Science,*
Beijing University of Technology, Beijing 100124, China

[3] *ARC Centre of Excellence for Particle Physics at the Terascale,*
School of Physics, The University of Sydney, NSW 2006, Australia

[4] *Key Laboratory of Theoretical Physics, Institute of Theoretical Physics,*
Chinese Academy of Sciences, Beijing 100190, China

Abstract

In this work, we explain the 750 GeV diphoton resonance in the Next-to-Minimal Supersymmetric Standard Model (NMSSM) by introducing vector-like particles. Such an extension is well motivated from the top-down view since some grand unified theories usually predict the existence of singlet scalars and vector-like particles at weak scale. In our model, the 750 GeV resonance can be interpreted as two nearly degenerate singlet-like Higgs bosons ($m_{h_2} \approx m_{a_1} \approx 750$ GeV). Under the constraints from the LHC data and dark matter experiments, we scan the parameter space and find that such a model can successfully account for the 750 GeV diphoton excess. Besides, we find that the two 750 GeV Higgs bosons h_2 and a_1 can sizably decay to $\chi_1^0\chi_1^0$ invisibly. Therefore, search for the monojet events through the process $gg \to h_2/a_1(\to \chi_1^0\chi_1^0)j$ can further test our scenario at the future LHC.

PACS numbers:

I. INTRODUCTION

Weak-scale supersymmetry (SUSY) resolves several problems in the Standard Model (SM), most notable of which is the gauge hierarchy problem [1], i.e. the difference between the electroweak scale and the Planck mass. A consequence of this theory is that the supersymmetric particles and the Higgs bosons should exist with masses typically less than 1 TeV. In fact, the discovery of the 125 GeV Higgs boson [2, 3] may be the first evidence of supersymmetry since it lies miraculously in the Higgs mass window $115-135$ GeV predicted by the Minimal Supersymmetric Standard Model (MSSM) [4]. So, if SUSY is indeed the new physics beyond the SM, more new particles could be found at the running or future LHC.

Intriguingly, both ATLAS data with 3.2 fb^{-1} [5] and CMS data with 2.6 fb^{-1} [6] have recently reported a diphoton resonance (X) around 750 GeV. The local significances of the signals are 3.6σ and 2.6σ in the respective experiments. The CMS collaboration has also performed a combination of their Run 1 and Run 2 data at $m_X \simeq 750$ GeV, finding that their significance can increase to right above 3σ. The compatibility of the signal hypothesis depends on the width of the resonance. The CMS data prefers a narrow resonance, while the ATLAS local significance varies from 3.6σ for a narrow width to 3.9σ for a broader resonance of $\Gamma_X/m_X \sim 6\%$. Up to now, many explanations have been proposed for explaining such an excess [7–15]. Among them, a feasible way is to introduce a singlet scalar as the 750 GeV resonance, which has no or very small couplings with the SM particles and decays to diphoton via loops of non-SM particles, in particular the vector-like fermions.

In fact, vector-like extensions are common in model buildings from the top-down approach. For example, vector-like particles can appear in certain GUT models, in extra-dimensional models or from the dimension deconstruction. The vector-like particles can also play an important role in SUSY breaking. For example, in some popular SUSY breaking models, such as SUGRA or gauge mediation supersymmetry breaking, the tree-level relation $m_{H_u}^2 = m_{H_d}^2$ will always be predicted. The electroweak symmetry breaking has to be driven by quantum corrections with such boundary conditions. In general, the large negative contributions to $m_{H_u}^2$ from the renormalization group equation (RGE) are important. If the boundary scale is low, the additional contributions from the heavy quarks to $m_{H_u}^2$ is welcome to successfully trigger the EWSB. The vector-like particles, which will not spoil the chiral structure of the MSSM, are the most natural extensions. Similar reasons hold for the NMSSM. So, we introduce vector-like particles in the NMSSM and allow them to couple with the singlet field.

In the NMSSM [16], the singlet field S is introduced to account for the notorious μ-problem [17]. After the EWSB, two singlet-like Higgs bosons (one is CP-even, the other is CP-odd) are obtained in the limit of small λ and each of them can serve as the 750 GeV resonance in the diphoton channel. Since the two singlet-like Higgs bosons are usually related and have certain mass splitting, so, in general, this will lead to two peaks in the diphoton invariant mass distribution, which is not favored by the current data. To reconcile with the observation, both singlet-like Higgs bosons should have degenerate masses or at least the mass splitting less than the detector resolution (the typical diphoton invariant mass resolution of the detector at 750 GeV is approximately ~ 10 GeV). Such a degenerate scenario has not been studied in the literature.

In this work, we interpret the 750 GeV diphoton reasonance as the degenerate singlet-like Higgs bosons in the NMSSM with vector-like particles. This paper is organized as follows. In Sec. II, we extend the NMSSM by introducing vector-like particles. In Sec. III we scan the parameter space and present the numerical results. Finally, the conculsion is given in Sec. IV.

II. NMSSM WITH VECTOR-LIKE PARTICLES

In the NMSSM, a singlet field S with coupling SH_uH_d is introduced and the μ-term is dynamically generated when S develops a vacuum expectation value (vev). In addition, the little hierarchy problem of the MSSM can be relaxed by the extra tree-level contributions to the SM-like Higgs boson mass. The Higgs superpotential of the NMSSM is given by [16],

$$W_{\mathrm{NMSSM}} = \lambda \widehat{S}\, \widehat{H}_u \cdot \widehat{H}_d + \frac{\kappa}{3}\widehat{S}^3 \qquad (1)$$

where λ and κ are dimensionless parameters. Then, a vev s of $\widehat{S}$ of the order of the weak or SUSY breaking scale generates an effective μ-term with

$$\mu_{\mathrm{eff}} = \lambda v_s \ , \qquad (2)$$

which solves the μ-problem of the MSSM. The full tree-level Higgs potential can be written as

$$\begin{aligned}
V^{(0,NMSSM)} &= (|\lambda S|^2 + m_{H_u}^2) H_u^\dagger H_u + (|\lambda S|^2 + m_{H_d}^2) H_d^\dagger H_d + m_S^2 |S|^2 \\
&+ \frac{1}{8}(g_2^2 + g_1^2)(H_u^\dagger H_u - H_d^\dagger H_d)^2 + \frac{1}{2} g_2^2 |H_u^\dagger H_d|^2 \\
&+ |\epsilon^{\alpha\beta} \lambda H_u^\alpha H_d^\beta + \kappa S^2|^2 + \left[\epsilon^{\alpha\beta} \lambda A_\lambda H_u^\alpha H_d^\beta S + \frac{1}{3}\kappa A_\kappa S^3 + \text{ h.c}\right], \qquad (3)
\end{aligned}$$

where A_λ and A_κ are the corresponding trilinear soft breaking parameters. To clearly see the properties of the Higgs sector, we expand the neutral scalar fields around the vevs as

$$\begin{aligned}
\mathrm{Re}\, H_d^0 &= (v_d - H\sin\beta + h\cos\beta)/\sqrt{2}, \quad \mathrm{Im}\, H_d^0 = (P\sin\beta + G^0\cos\beta)/\sqrt{2}, \\
\mathrm{Re}\, H_u^0 &= (v_u + H\cos\beta + h\sin\beta)/\sqrt{2}, \quad \mathrm{Im}\, H_u^0 = (P\cos\beta - G^0\sin\beta)/\sqrt{2}, \\
\mathrm{Re}\, S &= (v_s + s)/\sqrt{2}, \qquad\qquad\qquad\quad \mathrm{Im}\, S = P_S/\sqrt{2}. \qquad (4)
\end{aligned}$$

Substituting Eq. (4) into Eq. (3), we can obtain the tree-level mass matrix squared M_S^2 for the neutral Higgs bosons as

$$M^2 = \frac{1}{2}\begin{pmatrix} H, h, s \end{pmatrix} M_S^2 \begin{pmatrix} H \\ h \\ s \end{pmatrix} + \frac{1}{2}\begin{pmatrix} P, P_s \end{pmatrix} M_P^2 \begin{pmatrix} P \\ P_s \end{pmatrix}. \qquad (5)$$

The tree-level $M_{S\,ij}^2$ and $M_{P\,ij}^2$ are given by [18]

$$\begin{aligned}
M_{S\,11}^2 &= M_A^2 + (M_Z^2 - \frac{1}{2}\lambda^2 v^2)\sin^2 2\beta, & (6)\\
M_{S\,12}^2 &= -\frac{1}{2}(M_Z^2 - \frac{1}{2}\lambda^2 v^2)\sin 4\beta, & (7)\\
M_{S\,13}^2 &= -\sqrt{2}\lambda v \mu x \cot 2\beta, & (8)\\
M_{S\,22}^2 &= M_Z^2 \cos^2 2\beta + \frac{1}{2}\lambda^2 v^2 \sin^2 2\beta, & (9)\\
M_{S\,23}^2 &= \sqrt{2}\lambda v \mu (1 - x), & (10)\\
M_{S\,33}^2 &= 4\frac{\kappa^2}{\lambda^2}\mu^2 + \frac{\kappa}{\lambda} A_\kappa \mu + \frac{\lambda^2 v^2}{2} x - \frac{\kappa\lambda}{2} v^2 \sin 2\beta, & (11)\\
M_{P\,11}^2 &= M_A^2, & (12)\\
M_{P\,12}^2 &= \frac{1}{2}(M_A^2 \sin 2\beta - 3\lambda\kappa v_s^2) v/v_s, & (13)\\
M_{P\,22}^2 &= \frac{1}{4}(M_A^2 \sin 2\beta + 3\lambda\kappa v_s^2) v^2/v_s^2 \sin 2\beta - 3\kappa v_s A_\kappa/\sqrt{2}, & (14)
\end{aligned}$$

with

$$M_A^2 = \frac{\lambda v_s}{\sin 2\beta}\left(\sqrt{2}A_\lambda + \kappa v_s\right), \quad x = \frac{1}{2\mu}(A_\lambda + 2\frac{\kappa}{\lambda}\mu). \qquad (15)$$

Here, it should be noted that the mass parameter M_A in the NMSSM can become the mass of the pseudoscalar Higgs boson only in the MSSM limit ($\lambda, \kappa \to 0$ with the ratio κ/λ fixed). In the NMSSM, M_A can be traded by the soft parameter A_λ.

The CP-even and CP-odd Higgs mass eigenstates h_i ($i = 1, 2, 3$) and a_i ($i = 1, 2$) can be respectively obtained by diagonalizing M_S^2 and M_P^2 with the rotation matrices $\mathcal{O}$ and $\mathcal{O}'$:

$$\begin{aligned} h_i &= \mathcal{O}_{i\alpha} h_\alpha, \quad (h_\alpha = H, h, s), \quad \mathrm{diag}(m_{h_1}^2, m_{h_2}^2, m_{h_3}^2) = \mathcal{O} M_S^2 \mathcal{O}^T \\ a_i &= \mathcal{O}'_{i\alpha} P_\alpha, \quad (P_\alpha = P, P_s), \quad \mathrm{diag}(m_{a_1}^2, m_{a_2}^2) = \mathcal{O}' M_P^2 \mathcal{O}'^T \end{aligned} \tag{16}$$

Here the elements of the rotation matrices satisfy the following sum rules

$$\begin{aligned} \mathcal{O}_{1\alpha}^2 + \mathcal{O}_{2\alpha}^2 + \mathcal{O}_{3\alpha}^2 &= 1, \\ \mathcal{O}'^2_{1\alpha} + \mathcal{O}'^2_{2\alpha} &= 1. \end{aligned} \tag{17}$$

The mass eigenstates h_i and a_i are aligned by the masses $m_{h_1} \le m_{h_2} \le m_{h_3}$ and $m_{a_1} \le m_{a_2}$, respectively. The singlet components in a physical Higgs boson h_i (a_i) are determined by the rotation matrix elements $\mathcal{O}_{is}$ ($\mathcal{O}'_{is}$).

	SU(3)	SU(2)	U(1)
$\widehat{X}$	$\bar{3}$	1	$-\frac{2}{3}$
$\widehat{Y}$	3	1	$\frac{2}{3}$

TABLE I: The quantum number of the vector particles under the SM gauge group.

To explain the 750 GeV excess, we introduce vector multiplets X_i and Y_i with the gauge symmetry in Table I, where the subscript i denotes the generation of vector multiplets. Then, we can write the superpotential of the vector multiplets as

$$W_{\mathrm{vector}} = \sum_{i=1}^{n} \left(Y_{Vi} \widehat{Q} \cdot \widehat{H}_u \widehat{X}_i + \lambda_{R_i} \widehat{S} \widehat{t}_R \widehat{Y}_i + \lambda_{V_i} \widehat{S} \widehat{X}_i \widehat{Y}_i \right). \tag{18}$$

All other terms are same as in the NMSSM. For simplicity, we assume a common coupling λ_V for all generations of vector multiplets. The corresponding soft SUSY breaking terms are given by

$$\begin{aligned} -\mathcal{L}_{\mathrm{soft}} &= M_X^2 |X|^2 + M_Y^2 |Y|^2 \\ &\quad + \left(Y_V A_Y Q \cdot H_u X + \lambda_R A_R S t_R Y + \lambda_V A_V S X Y + B_V M_V X Y + \mathrm{H.c.} \right) \end{aligned} \tag{19}$$

For simplicity, we ignore the mixing between the newly added vector-like quark with the top quark by setting $Y_V, \lambda_R = 0$ in our following study. Then we can have the Dirac fermion

$$V = \begin{pmatrix} Y \\ \bar{X} \end{pmatrix}$$

with $m_V = \lambda_V v_s$. The coupling of $h_i \bar{V} V$ interaction is proportional to $\lambda_V \mathcal{O}_{3i}$. The mass matrix of the vector particle in the basis of $(X^*, Y)^T$ is given by (contribution from D-term have been ignored)

$$\begin{pmatrix} \lambda_V^2 v_s^2 + M_X^2 & \lambda_V \kappa v_s^2 + \lambda_V A_V v_s + B_V M_V - \lambda \lambda_V v_u v_d \\ \lambda_V \kappa v_s^2 + \lambda_V A_V v_s + B_V M_V - \lambda \lambda_V v_u v_d & \lambda_V^2 v_s^2 + M_Y^2 \end{pmatrix} \tag{20}$$

After diagonalizing Eq.(20) to mass eigenstate $(\tilde{V}_1, \tilde{V}_2)^T$ by the rotation matrix L, we have the coupling of $H_i \tilde{V}_j \tilde{V}_k^*$ in the mass eigenstates as

$$\begin{aligned} & 2\lambda_V^2 v_s \mathcal{O}_{3i}(L^{2j} L^{2k*} + L^{1j} L^{1k*}) + \lambda_V (2\kappa v_s + A_V) \mathcal{O}_{3i}(L^{2j} L^{1k*} + L^{1j} L^{2k*}) \\ & - \lambda \lambda_V v_d \mathcal{O}_{1i}(L^{2j} L^{1k*} + L^{1j} L^{2k*}) - \lambda \lambda_V v_u \mathcal{O}_{2i}(L^{2j} L^{1k*} + L^{1j} L^{2k*}) \end{aligned} \tag{21}$$

In the end, the newly introduced free model parameters are $\lambda_V, A_V, B_V, M_X^2, M_Y^2, M_V^2$.

III. NUMERICAL RESULTS AND DISCUSSIONS

To interpret the diphoton excess, the CMS and ATLAS experiments at the 13 TeV LHC approximately give the production rate of the resonance X [13]

$$\sigma_{\gamma\gamma}^{750}(\text{CMS}) = \sigma(pp \to X) \times Br(X \to \gamma\gamma) = 5.6^{+2.4}_{-2.4} fb, \tag{22}$$

$$\sigma_{\gamma\gamma}^{750}(\text{ATLAS}) = \sigma(pp \to X) \times Br(X \to \gamma\gamma) = 6.0^{+2.4}_{-2.0} fb. \tag{23}$$

Combined with the 8 TeV data, the diphoton excess contributing to the combined production rate is given by [13]

$$\sigma_{\gamma\gamma}^{750} = (4.6 \pm 1.2) \text{ fb} . \tag{24}$$

The new vector-like particles can contribute to the effective potential, which will significantly change the Higgs mass matrix and the loop-induced Higgs couplings, such as hgg and $h\gamma\gamma$. At one-loop, their contributions are given by

$$V_1 = \sum_i \frac{n_i M_i^4}{64\pi^2} \left[\log \frac{M_i^2}{\Lambda^2} - \frac{3}{2} \right] \tag{25}$$

where i denotes the mass eigenstate, $n_i = -12$ for fermions and $n_i = 6$ for scalars, and M_i^2 are the field-dependent masses. We modify the the package NMSSMTOOLS [19] to include the contributions of the vector-like particles. Then we scan the parameter space of our model in the following range

$$\begin{aligned}
0.0 < \lambda, \kappa < 0.7,\ 1.0 < \tan\beta < 15.0,\ 100\text{GeV} < \mu < 500\text{GeV},\ 0 < A_\lambda < 3\text{TeV}, \\
|A_\kappa| < 1\text{TeV},\ 500\text{GeV} < m_{U_3,Q_3} < 3\text{TeV},\ -3\text{TeV} < A_t < 3\text{TeV}, 0 < M_{1,2} < 2\text{TeV}, \\
0.0 < \lambda_V < 6,\ 0.1\text{TeV} < M_X = M_Y = M_V < 3\text{TeV},\ -4\text{TeV} < A_V, B_V < 4\text{TeV}. \quad (26)
\end{aligned}$$

The soft mass parameters for the first two generations and the slepton sector are set to 2 TeV and other trilinear soft terms are set to zero. The generation of vector-like particles are chosen as 3. We require our samples to explain the diphoton excess within the 2σ range of Eq.(24) and impose the following constraints:

(1) We require the SM-like Higgs mass in the range of 123-127 GeV and use the 95% exclusion limits from LEP, Tevatron and LHC in the Higgs searches with HiggsBounds-4.2.0 [20]. We also perform the Higgs data fit by calculating χ^2 of the Higgs couplings with the package HiggsSignals-1.3.0 [21] and require our samples to be consistent with the Higgs data at 2σ level.

(2) We require the two singlet-like CP-even and CP-odd Higgs bosons lie in the mass range 750 ± 5 GeV.

(3) In order to obtain a stable color vacuum, the bilinear part need to be positively definite and the trilinear terms cannot be too large:

$$|2M_V B_V| < M_X^2 + M_Y^2, \quad (27)$$

$$|A_V| < 2.5\sqrt{M_X^2 + M_Y^2 - |2M_V B_V|}. \quad (28)$$

(4) We require the thermal relic density of the lightest neutralino (as the dark matter candidate) is lower than the upper bound of the Planck value [22].

(5) The CMS search for a dijet resonance [23] at $\sqrt{s} = 8$ TeV with $\mathcal{L} = 18.8\ fb^{-1}$ gives a 95% C.L. upper limit:

$$\sigma(pp \to X)_{8\,\text{TeV}} \times Br(X \to gg) < 1.8 \text{ pb} \quad (29)$$

(6) The ATLAS [25] and CMS [26] searches for a scalar resonance decaying to $VV(V = W, Z)$ at $\sqrt{s} = 8$ TeV with the full data set, combining all relevant Z and W decay channels, give a 95% CL upper limit on the production of the scalar decaying to VV:

$$\sigma(pp \to S)_{8\,\mathrm{TeV}} \times \mathcal{B}(S \to ZZ) < 22\,\mathrm{fb}_{\,(\mathrm{ATLAS})}\,,\ 27\,\mathrm{fb}_{\,(\mathrm{CMS})}\,, \tag{30}$$

$$\sigma(pp \to S)_{8\,\mathrm{TeV}} \times \mathcal{B}(S \to WW) < 38\,\mathrm{fb}_{\,(\mathrm{ATLAS})}\,,\ 220\,\mathrm{fb}_{\,(\mathrm{CMS})}\,. \tag{31}$$

(7) Since the LSP masses can be lighter than 375 GeV, the Higgs bosons h_2 and a_1 can invisibly decay to the LSP, which will lead to the monojet signature $gg \to h_1/a_1(\to \chi_1^0\chi_1^0)j$. The CMS monojet analysis gives a limit on the invisible decay [24] at $\sqrt{s} = 8$ TeV LHC:

$$\sigma(pp \to X)_{8\,\mathrm{TeV}} \times Br(X \to invisible) < 0.8\ \mathrm{pb} \tag{32}$$

(8) The ATLAS [27] and CMS [28] searches for a resonance decaying to $\gamma\gamma$ at $\sqrt{s} = 8$ TeV give a 95% CL upper limit on the production cross section:

$$\sigma(pp \to X)_{8\,\mathrm{TeV}} \times Br(X \to \gamma\gamma) < 2.2\,\mathrm{fb}_{\,(\mathrm{ATLAS})}\,,\ 1.3\,\mathrm{fb}_{\,(\mathrm{CMS})}\,. \tag{33}$$

We calculate the production cross section of $gg \to h_2, a_1$ at the 13 TeV LHC by using the package HIGLU[29] with CTEQ6.6M PDFs [30]. We take the renormalization and factorization scales as $\mu_R = \mu_F = m_S/2$. We also include a K-factor $(1 + 67\alpha_s/4\pi)$ [31] in the calculation of the decay width of $S \to gg$.

In Table II, we present a benchmark point that can successfully explian the diphoton excess under the constraints (1)-(8). From this table we can see:

(1) The lightest CP-even Higgs boson h_1 is SM-like.

(2) The next-to-lightest CP-even Higgs boson h_2 and the lightest CP-odd Higgs boson a_1 have a similar mass around 750 GeV.

(3) The total decay widths of the CP-even and CP-odd singlet-like Higgs bosons are 12.8 GeV and 14.6 GeV, respectively.

(4) The dominant decay mode of h_2 is $h_2 \to gg$, while a_1 mainly decays to $\tilde{\chi}_1^+\tilde{\chi}_1^-$.

(5) The production cross sections of $gg \to h_2$ and $gg \to a_1$ can reach 6.9 pb and 7.7 pb, respectively. The branching ratios of $h_1(a_1) \to \gamma\gamma$ are about 0.022%. Then, the total production rate of the diphoton can be 3.22 fb.

TABLE II: A benchmark point in the NMSSM to explain the 750 GeV diphoton excess.

λ	κ	$\tan\beta$	μ (GeV)	A_λ (GeV)	A_κ (GeV)	m_{Q3} (GeV)
0.594	0.428	14.65	113.5	1908.5	-631.5	1855
m_{U3} (GeV)	A_t (GeV)	M_1 (GeV)	M_2(GeV)	N_f	λ_V	
1997	-2693.6	1984.81	512.19	3	5.06	
M_X (GeV)	A_V (GeV)	B_V (GeV)	m_{h1} (GeV)	m_{h2}(GeV)	m_{h3}(GeV)	
427.3	307.1	-96.12	124.36	745.7	1448.3	
m_{a1}(GeV)	m_{a2}(GeV)	$m_{h^\pm}$(GeV)	$m_{\tilde{\chi}_1^\pm}$(GeV)	$m_{\tilde{\chi}_1^0}$(GeV)	$m_{\tilde{\chi}_2^0}$(GeV)	$m_{\tilde{\chi}_3^0}$(GeV)
750.6	1775.0	1770.8	112.79	70.3	141.7	226.8
m_{V_F}(GeV)	$m_{V_{s_1}}$(GeV)	$m_{V_{s_2}}$(GeV)	$\mathcal{O}_{13}^2$	Ωh^2	$\sigma_{gg\to h_2}^{13TeV}$(fb)	$\Gamma(h_2)$(GeV)
968.8	893.1	1202.09	2.79×10^{-5}	0.0906	6885.8	12.8
$BR_{h_2\to\tau\tau}$	$BR_{h_2\to bb}$	$BR_{h_2\to tt}$	$BR_{h_2\to WW}$	$BR_{h_2\to ZZ}$	$BR_{h_2\to\gamma\gamma}$	$BR_{h_2\to Z\gamma}$
0.025%	0.174%	0.0006%	0.026%	0.014%	0.022%	0.013%
$BR_{h_2\to gg}$	$BR_{h_2\to h_1h_1}$	$BR_{h_2\to\tilde{\chi}_1^0\tilde{\chi}_1^0}$	$BR_{h_2\to\tilde{\chi}_1^0\tilde{\chi}_2^0}$	$BR_{h_2\to\tilde{\chi}_1^0\tilde{\chi}_3^0}$	$BR_{h_2\to\tilde{\chi}_2^0\tilde{\chi}_2^0}$	$BR_{h_2\to\tilde{\chi}_2^0\tilde{\chi}_3^0}$
6.8%	0.059%	22.7%	4.6%	0.98%	11.8%	6.1%
$BR_{h_2\to\tilde{\chi}_3^0\tilde{\chi}_3^0}$	$BR_{h_2\to\tilde{\chi}_1^\pm\tilde{\chi}_1^\pm}$	$\sigma_{gg\to a_1}^{13TeV}$(fb)	$\Gamma(a_1)$(GeV)	$BR_{a_1\to\tau\tau}$	$BR_{a_1\to bb}$	$BR_{a_1\to tt}$
14.3%	31.6%	7689.14	14.6	0.0098%	0.068%	0.0049%
$BR_{a_1\to WW}$	$BR_{a_1\to ZZ}$	$BR_{a_1\to\gamma\gamma}$	$BR_{a_1\to Z\gamma}$	$BR_{a_1\to gg}$	$BR_{a_1\to h_1Z}$	$BR_{a_1\to\tilde{\chi}_1^0\tilde{\chi}_1^0}$
0	0.0018%	0.022%	0.013%	6.7%	9.5×10^{-8}	16.9%
$BR_{a_1\to\tilde{\chi}_1^0\tilde{\chi}_2^0}$	$BR_{a_1\to\tilde{\chi}_1^0\tilde{\chi}_3^0}$	$BR_{a_1\to\tilde{\chi}_2^0\tilde{\chi}_2^0}$	$BR_{a_1\to\tilde{\chi}_2^0\tilde{\chi}_3^0}$	$BR_{a_1\to\tilde{\chi}_3^0\tilde{\chi}_3^0}$	$BR_{a_1\to\tilde{\chi}_1^\pm\tilde{\chi}_1^\pm}$	$\sigma_{\gamma\gamma}^{13TeV}$(fb)
4.3%	0.27%	10.8%	6.38%	22.3%	31.4%	3.22

In Fig.1, we plot the surviving samples on the plane of λ_V versus A_V. All the samples satisfy the constraints (1)-(8) and the 2σ range of Eq.(24). From Fig.1 we can see that when the Yukawa coupling λ_V becomes smaller, the trilinear parameter A_V should be larger and the higgsino mass μ tends to be lighter. Otherwise, the large λ_V and A_V will overly enhance the diphoton production rate and also give rise to the unacceptably huge correction to the 750 GeV heavy Higgs masses. The favorable ranges of λ_V and v_S are $4.4-5.8$ and $170\text{GeV}-225\text{GeV}$, respectively.

Due to the light LSP and higgsinos, the two 750 GeV Higgs bosons h_2 and a_1 can decay to $\chi_{1,2,3}^0$ and $\chi_1^+\chi_1^-$. In Fig.2 we present the decay branching ratios of h_2 and a_1. It can

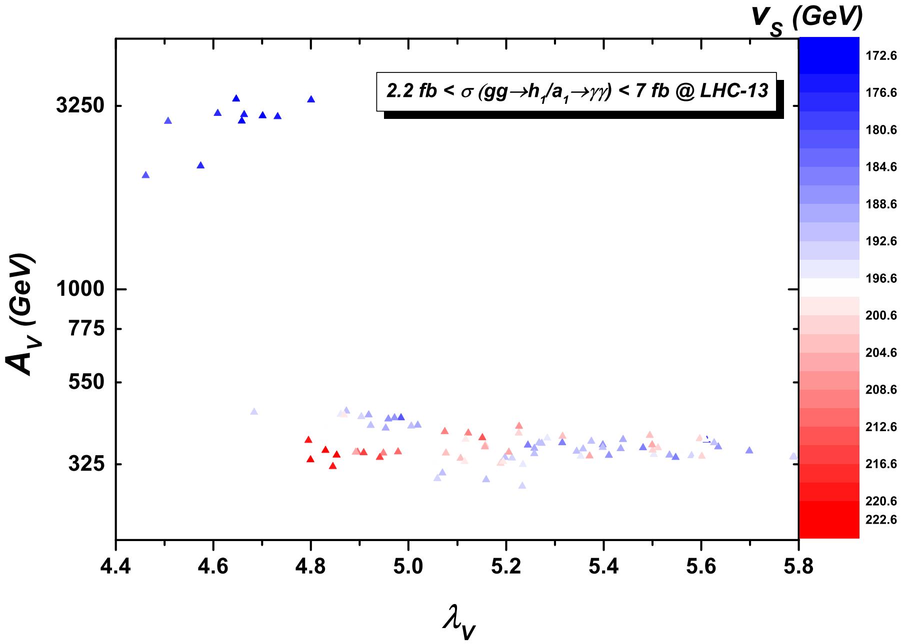

FIG. 1: Scatter plots of the survived samples on the plane of λ_V versus A_V. The color map corresponds to the values of v_S. All the samples satisfy the constraints (1)-(8) and the 2σ range of Eq.(24).

be seen that both h_2 and a_1 dominantly decay to $\chi_1^+\chi_1^-$ with a branching ratio $Br \simeq 40\%$. The invisible decay branching ratio of $h_2(a_1) \to \chi_1^0\chi_1^0$ can maximally reach about 30%(20%). Thus, the future search for the monojet events through the process $gg \to h_2/a_1(\to \chi_1^0\chi_1^0)j$ can further test our scenario.

IV. CONCLUSIONS

We interpreted the 750 GeV diphoton resonance in the NMSSM by introducing vector-like particles. In our model, the 750 GeV resonance was interpreted as two nearly degenerate singlet-like Higgs bosons ($m_{h_2} \approx m_{a_1} \approx 750$ GeV). The decays of $h_2(a_1) \to \gamma\gamma$ are dominated by the vector-like squarks with small singlet vev v_S, which can also enhance the production cross section of $gg \to h_2/a_1$. Under the current LHC constraints and the dark matter detection limits, we scanned the parameter space and found that such a scenario can successfully account for the diphoton excess. On the other hand, we noticed that the two 750 GeV resonances h_2 and a_1 have sizable invisible decay branching ratio $h_2(a_1) \to \chi_1^0\chi_1^0$. Therefore, the future search for the monojet events through the process $gg \to h_2/a_1(\to \chi_1^0\chi_1^0)j$ can

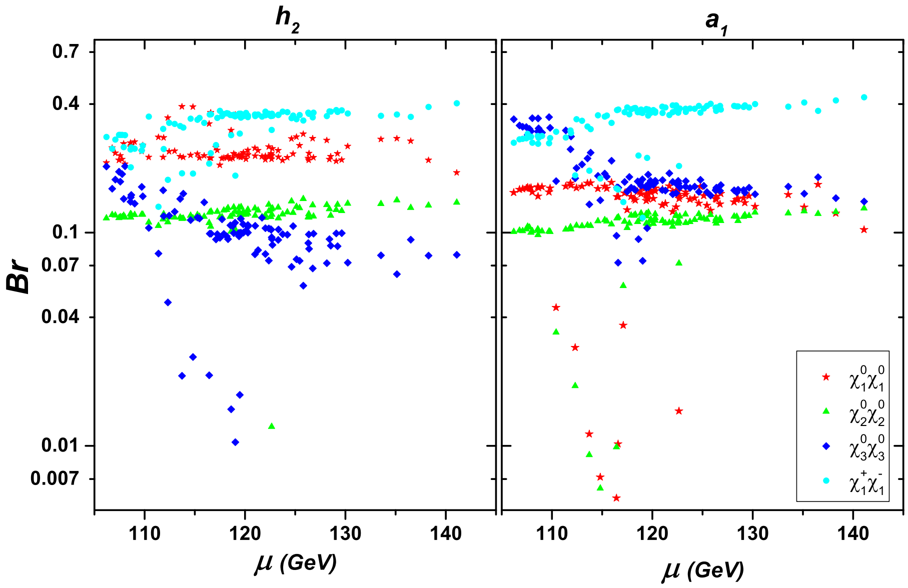

FIG. 2: Same as Fig.1, but showing the decay branching ratios of h_2 (left panel) and a_1 (right panel) versus the higgsino mass parameter μ.

further test our scenario at the LHC.

Acknowledgments

This work is partly supported by the Australian Research Council, by the National Natural Science Foundation of China (NNSFC) under grants Nos. 11105124,11105125,11275057, 11305049, 11375001, 11405047, 11135003, 11275245, by Specialised Research Fund for the Doctoral Program of Higher Education under Grant No. 20134104120002; by the Open Project Program of State Key Laboratory of Theoretical Physics, Institute of Theoretical Physics, Chinese Academy of Sciences (No.Y5KF121CJ1); by the Innovation Talent project of Henan Province under grant number 15HASTIT017; by the Joint Funds of the National Natural Science Foundation of China (U1404113); by the Young-Talent Foundation of Zhengzhou University; by Ri-Xin Foundation of BJUT, and by the CAS Center for Excellence in Particle Physics (CCEPP).

---

[1] S. Dimopoulos and H. Georgi, Nucl. Phys. **B193** (1981) 150; N. Sakai, Z. Phys. **C11** (1981) 153.

[2] G. Aad *et al.* [ATLAS Collaboration], Phys. Lett. B **716**, 1 (2012).

[3] S. Chatrchyan *et al.* [CMS Collaboration], Phys. Lett. B **716**, 30 (2012).

[4] For a review, see, e.g., H. E. Haber and G. L. Kane, Phys. Rept. **117**, 75 (1985).

[5] CMS Collaboration [CMS Collaboration], CMS-PAS-EXO-15-004.

[6] The ATLAS collaboration [ATLAS Collaboration], ATLAS-CONF-2015-081.

[7] D. Buttazzo, A. Greljo and D. Marzocca, arXiv:1512.04929 [hep-ph].

[8] Y. Mambrini, G. Arcadi and A. Djouadi, arXiv:1512.04913 [hep-ph]; A. Pilaftsis, arXiv:1512.04931 [hep-ph]; R. Franceschini *et al.*, arXiv:1512.04933 [hep-ph]; S. Di Chiara, L. Marzola and M. Raidal, arXiv:1512.04939 [hep-ph]; K. Harigaya and Y. Nomura, arXiv:1512.04850 [hep-ph]; M. Backovic, A. Mariotti and D. Redigolo, arXiv:1512.04917 [hep-ph]; A. Angelescu, A. Djouadi and G. Moreau, arXiv:1512.04921 [hep-ph]; Y. Nakai, R. Sato and K. Tobioka, arXiv:1512.04924 [hep-ph]; S. Knapen, T. Melia, M. Papucci and K. Zurek, arXiv:1512.04928 [hep-ph].

[9] T. Higaki, K. S. Jeong, N. Kitajima and F. Takahashi, arXiv:1512.05295 [hep-ph]; S. D. McDermott, P. Meade and H. Ramani, arXiv:1512.05326 [hep-ph]; J. Ellis, S. A. R. Ellis, J. Quevillon, V. Sanz and T. You, arXiv:1512.05327 [hep-ph]; M. Low, A. Tesi and L. T. Wang, arXiv:1512.05328 [hep-ph]; B. Bellazzini, R. Franceschini, F. Sala and J. Serra, arXiv:1512.05330 [hep-ph]; R. S. Gupta, S. Jger, Y. Kats, G. Perez and E. Stamou, arXiv:1512.05332 [hep-ph]; C. Petersson and R. Torre, arXiv:1512.05333 [hep-ph]; E. Molinaro, F. Sannino and N. Vignaroli, arXiv:1512.05334 [hep-ph].

[10] D. Aloni, K. Blum, A. Dery, A. Efrati and Y. Nir, arXiv:1512.05778 [hep-ph]; A. Falkowski, O. Slone and T. Volansky, arXiv:1512.05777 [hep-ph]; C. Csaki, J. Hubisz and J. Terning, arXiv:1512.05776 [hep-ph]; J. Chakrabortty, A. Choudhury, P. Ghosh, S. Mondal and T. Srivastava, arXiv:1512.05767 [hep-ph]; L. Bian, N. Chen, D. Liu and J. Shu, arXiv:1512.05759 [hep-ph]; D. Curtin and C. B. Verhaaren, arXiv:1512.05753 [hep-ph]; S. Fichet, G. von Gersdorff and C. Royon, arXiv:1512.05751 [hep-ph]; W. Chao, R. Huo and J. H. Yu, arXiv:1512.05738 [hep-ph]; S. V. Demidov and D. S. Gorbunov, arXiv:1512.05723 [hep-ph]; J. M. No, V. Sanz and J. Setford, arXiv:1512.05700 [hep-ph]; D. Becirevic, E. Bertuzzo, O. Sumensari and R. Z. Funchal, arXiv:1512.05623 [hep-ph]; R. Martinez, F. Ochoa and C. F. Sierra, arXiv:1512.05617 [hep-ph]; P. Agrawal, J. Fan, B. Heidenreich, M. Reece and M. Strassler, arXiv:1512.05775 [hep-ph]; A. Ahmed, B. M. Dillon, B. Grzadkowski,

J. F. Gunion and Y. Jiang, arXiv:1512.05771 [hep-ph]; P. Cox, A. D. Medina, T. S. Ray and A. Spray, arXiv:1512.05618 [hep-ph]; S. Matsuzaki and K. Yamawaki, arXiv:1512.05564 [hep-ph]; Q. H. Cao, Y. Liu, K. P. Xie, B. Yan and D. M. Zhang, arXiv:1512.05542 [hep-ph]; B. Dutta, Y. Gao, T. Ghosh, I. Gogoladze and T. Li, arXiv:1512.05439 [hep-ph].

[11] E. Gabrielli, K. Kannike, B. Mele, M. Raidal, C. Spethmann and H. Veerm?e, arXiv:1512.05961 [hep-ph]; R. Benbrik, C. H. Chen and T. Nomura, arXiv:1512.06028 [hep-ph]; J. S. Kim, J. Reuter, K. Rolbiecki and R. R. de Austri, arXiv:1512.06083 [hep-ph]; J. Bernon and C. Smith, arXiv:1512.06113 [hep-ph]; E. Megias, O. Pujolas and M. Quiros, arXiv:1512.06106 [hep-ph]; A. Alves, A. G. Dias and K. Sinha, arXiv:1512.06091 [hep-ph]; L. M. Carpenter, R. Colburn and J. Goodman, arXiv:1512.06107 [hep-ph].

[12] D. Barducci, A. Goudelis, S. Kulkarni and D. Sengupta, arXiv:1512.06842 [hep-ph]; M. Chala, M. Duerr, F. Kahlhoefer and K. Schmidt-Hoberg, arXiv:1512.06833 [hep-ph]; M. Bauer and M. Neubert, arXiv:1512.06828 [hep-ph]; J. M. Cline and Z. Liu, arXiv:1512.06827 [hep-ph]; W. S. Cho, D. Kim, K. Kong, S. H. Lim, K. T. Matchev, J. C. Park and M. Park, arXiv:1512.06824 [hep-ph]; L. Berthier, J. M. Cline, W. Shepherd and M. Trott, arXiv:1512.06799 [hep-ph]; J. S. Kim, K. Rolbiecki and R. R. de Austri, arXiv:1512.06797 [hep-ph]; X. J. Bi, Q. F. Xiang, P. F. Yin and Z. H. Yu, arXiv:1512.06787 [hep-ph]; M. Dhuria and G. Goswami, arXiv:1512.06782 [hep-ph]; J. J. Heckman, arXiv:1512.06773 [hep-ph]; W. Liao and H. q. Zheng, arXiv:1512.06741 [hep-ph]; F. P. Huang, C. S. Li, Z. L. Liu and Y. Wang, arXiv:1512.06732 [hep-ph]; J. Cao, C. Han, L. Shang, W. Su, J. M. Yang and Y. Zhang, arXiv:1512.06728 [hep-ph]; F. Wang, L. Wu, J. M. Yang and M. Zhang, arXiv:1512.06715 [hep-ph]; T. F. Feng, X. Q. Li, H. B. Zhang and S. M. Zhao, arXiv:1512.06696 [hep-ph]; D. Bardhan, D. Bhatia, A. Chakraborty, U. Maitra, S. Raychaudhuri and T. Samui, arXiv:1512.06674 [hep-ph]; J. Chang, K. Cheung and C. T. Lu, arXiv:1512.06671 [hep-ph]; M. x. Luo, K. Wang, T. Xu, L. Zhang and G. Zhu, arXiv:1512.06670 [hep-ph]; X. F. Han and L. Wang, arXiv:1512.06587 [hep-ph]; H. Han, S. Wang and S. Zheng, arXiv:1512.06562 [hep-ph]; R. Ding, L. Huang, T. Li and B. Zhu, arXiv:1512.06560 [hep-ph]; I. Chakraborty and A. Kundu, arXiv:1512.06508 [hep-ph]; C. Han, H. M. Lee, M. Park and V. Sanz, arXiv:1512.06376 [hep-ph]; M. T. Arun and P. Saha, arXiv:1512.06335 [hep-ph]; W. Chao, arXiv:1512.06297 [hep-ph].

[13] P. S. B. Dev and D. Teresi, arXiv:1512.07243 [hep-ph]; A. Belyaev, G. Cacciapaglia, H. Cai,

T. Flacke, A. Parolini and H. Serodio, arXiv:1512.07242 [hep-ph]; J. de Blas, J. Santiago and R. Vega-Morales, arXiv:1512.07229 [hep-ph]; G. M. Pelaggi, A. Strumia and E. Vigiani, arXiv:1512.07225 [hep-ph]; U. K. Dey, S. Mohanty and G. Tomar, arXiv:1512.07212 [hep-ph]; A. E. C. Hernandez and I. Nisandzic, arXiv:1512.07165 [hep-ph]; C. W. Murphy, arXiv:1512.06976 [hep-ph]; S. M. Boucenna, S. Morisi and A. Vicente, arXiv:1512.06878 [hep-ph].

[14] J. Gu and Z. Liu, arXiv:1512.07624 [hep-ph]; M. Cvetic, J. Halverson and P. Langacker, arXiv:1512.07622 [hep-ph]; W. Altmannshofer, J. Galloway, S. Gori, A. L. Kagan, A. Martin and J. Zupan, arXiv:1512.07616 [hep-ph]; Q. H. Cao, S. L. Chen and P. H. Gu, arXiv:1512.07541 [hep-ph]; S. Chakraborty, A. Chakraborty and S. Raychaudhuri, arXiv:1512.07527 [hep-ph]; M. Badziak, arXiv:1512.07497 [hep-ph]; K. M. Patel and P. Sharma, arXiv:1512.07468 [hep-ph]; S. Moretti and K. Yagyu, arXiv:1512.07462 [hep-ph]; W. C. Huang, Y. L. S. Tsai and T. C. Yuan, arXiv:1512.07268 [hep-ph].

[15] L. J. Hall, K. Harigaya and Y. Nomura, arXiv:1512.07904 [hep-ph]; J. A. Casas, J. R. Espinosa and J. M. Moreno, arXiv:1512.07895 [hep-ph]; J. Zhang and S. Zhou, arXiv:1512.07889 [hep-ph]; J. Liu, X. P. Wang and W. Xue, arXiv:1512.07885 [hep-ph]; K. Cheung, P. Ko, J. S. Lee, J. Park and P. Y. Tseng, arXiv:1512.07853 [hep-ph]; K. Das and S. K. Rai, arXiv:1512.07789 [hep-ph]; H. Davoudiasl and C. Zhang, arXiv:1512.07672 [hep-ph]; B. C. Allanach, P. S. B. Dev, S. A. Renner and K. Sakurai, arXiv:1512.07645 [hep-ph]; N. Craig, P. Draper, C. Kilic and S. Thomas, arXiv:1512.07733 [hep-ph].

[16] U. Ellwanger, C. Hugonie and A. M. Teixeira, Phys. Rept. **496**, 1 (2010) [arXiv:0910.1785 [hep-ph]]; J. Cao, *et al.*, JHEP **1203**, 086 (2012) [arXiv:1202.5821 [hep-ph]].

[17] J. E. Kim and H.P. Nilles, Phys. Lett. **B138** (1984) 150.

[18] D. J. Miller, R. Nevzorov and P. M. Zerwas, Nucl. Phys. B **681**, 3 (2004) [hep-ph/0304049]; R. Nevzorov and D. J. Miller, hep-ph/0411275.

[19] U. Ellwanger, J. F. Gunion and C. Hugonie, JHEP 0502(2005) 006; U. Ellwanger and C. Hugonie, Comput. Phys. Commun. 175 (2006) 290; G. Belanger *et al.*, JCAP 0509:001 (2005).

[20] P. Bechtle, *et al.*, Comput. Phys. Commun. **182**, 2605 (2011); Comput. Phys. Commun. **181**, 138 (2010).

[21] P. Bechtle *et al.*, Eur. Phys. J. C **74**, 2711 (2014) [arXiv:1305.1933 [hep-ph]]; Comput. Phys. Commun. **181**, 138 (2010) [arXiv:0811.4169 [hep-ph]].

[22] P. A. R. Ade *et al.* [Planck Collaboration], arXiv:1303.5076 [astro-ph.CO].

[23] CMS Collaboration [CMS Collaboration], CMS-PAS-EXO-14-005.

[24] V. Khachatryan *et al.* [CMS Collaboration], Eur. Phys. J. C **75**, no. 5, 235 (2015) doi:10.1140/epjc/s10052-015-3451-4 [arXiv:1408.3583 [hep-ex]].

[25] G. Aad et al. [ATLAS Collaboration], arXiv:1507.05930 [hep-ex]; arXiv:1509.00389 [hep-ex].

[26] V. Khachatryan et al. [CMS Collaboration], JHEP 1510, 144 (2015).

[27] CMS Collaboration [CMS Collaboration], CMS-PAS-HIG-14-006.

[28] G. Aad et al. [ATLAS Collaboration], Phys. Rev. D 92, no. 3, 032004 (2015) [arXiv:1504.05511 [hep-ex]].

[29] M. Spira, hep-ph/9510347.

[30] D. Stump *et al.*, JHEP **0310**, 046 (2003) [hep-ph/0303013].

[31] M. Spira, A. Djouadi, D. Graudenz and P.M. Zerwas, Nucl. Phys. B453 (1995) 17; T. Inami, T. Kubota and Y. Okada, Z. Phys. C18 (1983) 69; A. Djouadi, M. Spira and P.M. Zerwas, Phys. Lett. B264 (1991) 440; M. Spira, A. Djouadi, D. Graudenz and P.M. Zerwas, Phys. Lett. B318 (1993) 347; S. Dawson and R.P. Kauffman, Phys. Rev. D49 (1994) 2298.